Article

Molecular Determinants of Mechanical Properties of *V. cholerae* Biofilms at the Air-Liquid Interface

Emily C. Hollenbeck,[1] Jiunn C. N. Fong,[2] Ji Youn Lim,[3] Fitnat H. Yildiz,[2] Gerald G. Fuller,[1] and Lynette Cegelski[3,*]
[1]Department of Chemical Engineering, Stanford University, Stanford, California; [2]Department of Microbiology and Environmental Toxicology, UC Santa Cruz, Santa Cruz, California; and [3]Department of Chemistry, Stanford University, Stanford, California

ABSTRACT Biofilm formation increases both the survival and infectivity of *Vibrio cholerae*, the causative agent of cholera. *V. cholerae* is capable of forming biofilms on solid surfaces and at the air-liquid interface, termed pellicles. Known components of the extracellular matrix include the matrix proteins Bap1, RbmA, and RbmC, an exopolysaccharide termed *Vibrio* polysaccharide, and DNA. In this work, we examined a rugose strain of *V. cholerae* and its mutants unable to produce matrix proteins by interfacial rheology to compare the evolution of pellicle elasticity in real time to understand the molecular basis of matrix protein contributions to pellicle integrity and elasticity. Together with electron micrographs, visual inspection, and contact angle measurements of the pellicles, we defined distinct contributions of the matrix proteins to pellicle morphology, microscale architecture, and mechanical properties. Furthermore, we discovered that Bap1 is uniquely required for the maintenance of the mechanical strength of the pellicle over time and contributes to the hydrophobicity of the pellicle. Thus, Bap1 presents an important matrix component to target in the prevention and dispersal of *V. cholerae* biofilms.

INTRODUCTION

Vibrio cholerae, the causative agent of cholera, survives in both aquatic ecosystems and in the small intestine of a human host (1–4). It is capable of forming biofilms, which are surface-associated communities of microorganisms enveloped in an extracellular matrix of secreted biopolymers (5,6). The biofilm lifestyle confers several advantages to a community of microorganisms, including increased resistance to antibiotics and protection from environmental stresses (7,8). Biofilms may enhance the ability of *V. cholerae* to survive in aquatic ecosystems, supporting seasonal outbreaks of cholera (7,9), and contribute to infectivity in the host (10). Thus, biofilm formation is important in aquatic habitats and in the human host, and the ability to interfere with biofilm formation could be instrumental in combating the severity of cholera outbreaks.

Improved models of biofilm assembly, structure, and function are needed to drive molecular strategies to interfere with *V. cholerae* biofilm formation. Several components of the *V. cholerae* biofilm matrix have been identified and include three proteins—RbmA, Bap1, and RbmC—and a polysaccharide termed *Vibrio* polysaccharide (5,11–13). The temporal production and spatial organization of these components at the cell surface and in the extracellular matrix of the rugose strain of *V. cholerae* grown on a solid substrate have been examined by immunofluorescence and super-resolution microscopy (14). The matrix protein RbmA provides cell-to-cell adhesion and is present in the early stages of biofilm formation, whereas the proteins Bap1 and RbmC appear later in development, and together with *Vibrio* polysaccharide encase clusters of cells. Additionally, Bap1 is localized near the biofilm-substrate interface and appears to anchor the biofilm to the solid surface. Complementary work with a smooth strain of *V. cholerae* additionally reported that RbmA is distributed uniformly throughout the biofilm (15). Collectively, we have a model of *V. cholerae* matrix formation that includes insight into the structural roles of important matrix proteins for biofilms formed on a solid surface. Yet, much less is known about the function of these proteins during pellicle formation and their contributions to the mechanical properties of the film at the air-liquid interface—the focus of this work.

The molecular composition and structure of a material are responsible for its mechanical properties. Thus, the measurement of mechanical properties often provides insight into microstructural differences between materials. Interfacial rheology has been used extensively to study complex fluid interfaces formed by surfactants, particles, polymers, biomolecules, and other materials (16–19) and has emerged as a powerful tool to measure the evolution of the mechanical properties of bacterial biofilms, including changes in the viscoelasticity of the film, in real time. We recently examined the specific contributions of functional amyloid fibers termed curli to biofilm formation in uropathogenic *Escherichia coli* and discovered that increased curli production increased the mechanical strength and elasticity of the pellicle and enhanced the ability to recover from physical perturbation (20,21). These results correlated molecular composition with macroscopic mechanical properties and

Submitted July 25, 2014, and accepted for publication October 1, 2014.

*Correspondence: cegelski@stanford.edu

Editor: James Cole.

0006-3495/14/11/2245/8 $2.00

http://dx.doi.org/10.1016/j.bpj.2014.10.015

function and revealed the importance of curli in the development and maintenance of the film elasticity. An important survey of many bacterial species revealed that pellicle mechanical properties can differ dramatically and change as a function of environmental factors such as temperature, pH, and nutrient availability (22). Thus, bacterial pellicles exhibit diverse mechanical properties that ultimately result from differences in the composition and structure of the extracellular matrix.

In this study, we implemented an integrated approach using interfacial rheology measurements, electron microscopy, and molecular profiling to examine the macroscopic and microstructural properties of pellicles formed by a rugose strain of *V. cholerae* and mutants unable to produce matrix proteins singly or in combination. We defined distinct contributions of the matrix proteins to pellicle morphology, microscale architecture, and the mechanical properties of the pellicles. Furthermore, we discovered that Bap1 is uniquely important for the integrity of pellicle structure and the maintenance of pellicle strength at the air-liquid interface. These findings underscore the importance of targeting Bap1 in efforts to develop biofilm inhibitors in *V. cholerae*.

MATERIALS AND METHODS

Bacterial strains

For all experiments, the rugose strain of *V. cholerae* O1 El Tor A1552 and RΔ*rbmA*, RΔ*rbmC*, RΔ*bap1*, RΔ*bap1*Δ*rbmC*, RΔ*rbmA*Δ*rbmC*, RΔ*rbmA*Δ*bap1*, RΔ*rbmA*Δ*bap1*Δ*rbmC* were used. RΔ*rbmA*Δ*rbmC*, RΔ*rbmA*Δ*bap1* double mutants were generated according to previous published protocols (11).

Cells were grown as overnight starter cultures in 4 mL Luria-Bertani (LB) medium at 37°C with 200 rpm shaking. Pellicles were then formed from a 1:1000 dilution of this overnight culture in LB medium at 26°C unless otherwise noted.

Western blot analyses

To determine RbmA, Bap1, and RbmC production in pellicle and planktonic samples, Western blot experiments were carried out similar to a previously described protocol (14). Briefly, pellicle and planktonic (1 ml) samples were harvested, resuspended in 2% sodium dodecyl sulfate and 10 μg of proteins were subjected to sodium dodecyl sulfate-polyacrylamide gel electrophoresis and Western blot analyses. Primary polyclonal rabbit α-RbmA and α-RbmC (1:1000) sera, secondary goat α-rabbit IgG-HRP (Santa Cruz Biotechnology, Dallas, TX, 1:2500), SuperSignal West Pico Chemiluminescent Substrate (Thermo Scientific, Waltham, MA), and a BioRad ChemiDoc MP Imaging System (Bio-Rad, Hercules, CA) were used for detection and capturing of the Western blot signals. It should be noted that α-RbmC serum (courtesy of S. Wai) also recognizes Bap1.

Interfacial rheology

The viscoelastic properties of the interface during pellicle formation were monitored using an AR-G2 rheometer (TA Instruments, New Castle, DE) with a du Noüy ring attachment made of Pt/Ir wire. During measurements, the du Noüy ring is positioned at the air-liquid interface in the inner chamber of a modified double-wall couette Teflon flow cell (Fig. 1, *A* and *B*). The standard double-wall ring arrangement was described previously (23). The flow cell rests on a plate maintained at 26°C and contains bacterial cells growing in nutrient broth. The timescales for pellicle formation are long and the flow cell for the double-wall ring required a special design to accommodate evaporation that can otherwise alter the position of the interface. The modified flow cell enables the continuous addition of fresh nutrient broth into the subphase of the inner chamber to adjust for evaporative loss and maintain the height of the air-liquid interface during the long-time course of pellicle formation. To initiate experiments, 30 mL of LB medium is added to the inner and outer chambers of the flow cell, and 10 µL of an overnight culture of bacteria is added to the inner chamber. Fresh media is introduced into the outer chamber at a rate of 0.5 mL/h using a 60 mL syringe and pump to adjust for evaporative losses and excess media is aspirated from the outer chamber at a specified height. A small hole connects the inner and outer chambers of the flow cell, allowing maintenance of a steady liquid level in the inner chamber without perturbing pellicle formation. During pellicle growth, the du Noüy ring oscillates about its circular axis with an angular frequency of 0.5 rad/s and at 1% strain in 10-min intervals. The torque required to oscillate the du Noüy ring and its angular displacement are used to calculate the shear stress and strain applied at the interface; the elastic and viscous moduli are calculated from this stress-strain relationship. The elastic interfacial moduli of the rugose pellicle, measured using three separate strain amplitudes, are shown in Fig. 1 *C*. These data establish that the strain amplitudes used in this study do not perturb the growth of the pellicle as the overall evolution and the local maxima are largely independent of strain. Only the elastic modulus is plotted as the *V. cholerae* pellicle is primarily elastic after 2–3 h of growth, consistent with previous biofilm studies (20–22,24,25).

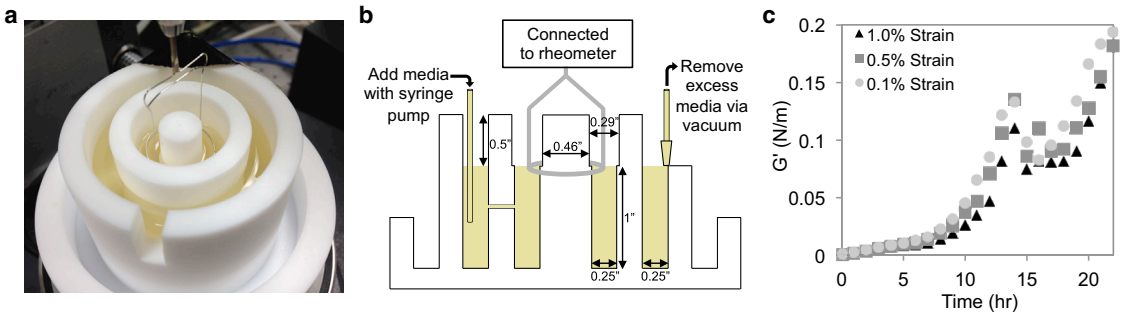

FIGURE 1 (*a*) The modified double wall-ring flow cell. The Teflon flow cell is filled with media and the du Noüy ring is positioned at the air-liquid interface. (*b*) Schematic of the experimental setup. Media is added to the outer chamber to account for evaporative losses during the experiment. Excess media is aspirated from the outer chamber at a specific height to maintain the liquid level in both the inner and outer chambers throughout the experiment without disturbing the pellicle. (*c*) The elastic interfacial moduli of the rugose pellicle as a function of time measured using three different strain amplitudes. The reproducibility of the data confirms that the strain amplitudes used in this study do not perturb the formation of the pellicle. To see this figure in color, go online.

Scanning electron microscopy (SEM)

Pellicles of the rugose strain and RΔ*rbmA*, RΔ*rbmC*, RΔ*bap1*, RΔ*bap1*Δ*rbmC*, RΔ*rbmA*Δ*rbmC*, RΔ*rbmA*Δ*bap1*, RΔ*rbmA*Δ*bap1* Δ*rbmC* mutants were grown in LB medium in a 12-well dish for 48 h at 26°C. Pellicles were then transferred to a fixative solution (2% glutaraldehyde, 4% formaldehyde in 0.1 M Na-Cacodylate, pH 7.4) and left overnight at 4°C. After fixation, the pellicles were washed for 10 min in 0.1 M Na-Cacodylate buffer (pH 7.4), followed by a postfixation step in 1% aqueous osmium tetroxide in 0.1 M Na-Cacodylate buffer (pH 7.4) for 1 h at 4°C. After another wash, the pellicles were dehydrated using successive ethanol treatments of 50%, 70%, 95%, and 100% ethanol, each lasting 10 min. Ethanol was removed from the pellicles using a critical point dryer and the dry pellicles were coated with gold-palladium. Low magnification images were captured using a Hitachi S-3400N scanning electron microscope, whereas higher magnification images were captured on a Zeiss Sigma scanning electron microscope.

Pellicle transfer assay

Pellicles were grown in a 24-well dish in LB medium for 48 h at 26°C. The pellicles were imaged using a Leica MC120 HD digital camera (Leica Microsystems, Buffalo Grove, IL) attached to a Leica S6D stereomicroscope. The pellicles were then transferred to a 24-well dish containing deionized water and again imaged.

Contact angle measurements

Pellicles were grown in a 12-well dish in LB medium for 48 h at 26°C. The pellicles were removed from the 12-well dish and spread flat on a glass microscope slide covered in water with the liquid-facing side of the pellicle touching the glass to maintain the same orientation of the pellicle, then left overnight to dry. An FTA1000B Drop Shape Analyzer (First Ten Angstroms, Portsmouth, VA) was used to make the contact angle measurements. Briefly, a droplet of water ~1 μL in volume was dropped on the surface of the pellicle. The drop was imaged from the side and FTA Drop Shape Analysis software was used to extract the angle between the air-liquid interface and the solid surface.

RESULTS

Molecular determinants of macroscale pellicle morphology and elasticity

To visualize macroscopic morphology in correlation with measurements of mechanical properties, pellicles were grown in the same Teflon flow cells used to perform rheological measurements (Fig. 1, *A* and *B*). Pellicles formed by rugose *V. cholerae* and individual *rbmA*, *bap1*, and *rbmC* mutants exhibit clear pellicles by visual inspection after 10 h (Fig. 2 *A*). Compared to the morphological evolution of the rugose pellicle, the RΔ*rbmA* pellicle is smoother in appearance and does not exhibit features of the mature pellicle until 35 h, whereas the evolution of the rugose pellicle appears more constant and exhibits features of the mature pellicle as early as 14 h. The RΔ*rbmC* pellicle morphology is similar to rugose, and the RΔ*bap1* pellicle differs in having a less intact wave-like appearance and finer, shallower wrinkles.

We performed measurements of the elastic modulus over the entire time course of pellicle formation to provide a more quantitative and physically informative understanding of the observed differences in pellicle formation. The elastic modulus describes the solid-like quality of the material, with a larger elastic modulus corresponding to a stiffer material. A pellicle has a heterogeneous structure, thus the moduli we report are effective moduli and were reproducible across triplicate measurements. As seen in Fig. 2, the elastic moduli of rugose and single mutant samples increase gradually for the first 10 h after inoculation, consistent with the colonization of bacteria at the air-liquid interface (20,26) and early production of extracellular matrix material, and then begin to increase more rapidly. Between 15 and 25 h, the elastic moduli of the rugose and single mutant pellicles exhibit a local maximum.

RbmA

The evolution of the elastic modulus of RΔ*rbmA* is delayed relative to the rugose pellicle (Fig. 2 *B*). The rugose elastic modulus reaches a local maximum at ~14 h, whereas the RΔ*rbmA* elastic modulus does not reach a local maximum until 22 h. The rate of increase in the RΔ*rbmA* elastic modulus is also slightly slower than rugose between 10 and 20 h. These trends are consistent with the visual observations of the macroscopic pellicles (Fig. 2 *A*): early pellicles are visible after 10 h, the rugose pellicle is considerably wrinkled at 14 h, yet the RΔ*rbmA* pellicle does not wrinkle until after 20 h. Thus, pellicles formed by bacteria lacking RbmA are delayed in development and reach a lower elastic modulus than rugose after 30 h.

Bap1

The evolution of the elastic modulus of the RΔ*bap1* pellicle is similar to rugose for the first 14 h and reaches a local maximum at ~14 h. However, the RΔ*bap1* elastic modulus subsequently decreases and remains diminished for the remainder of the experiment. Thus, these results provide a quantitative physicochemical basis for considering the visual observations in Fig. 2 *A* and suggest that Bap1 is important in maintaining the mechanical strength of the pellicle and likely plays a significant architectural role.

RbmC

The matrix protein RbmC is found around microcolonies within the *V. cholerae* biofilm grown on a solid surface (14). However, mutants lacking RbmC do not exhibit significant change in pellicle morphology (12). Our measurements show that a deficiency in RbmC does not significantly affect the evolution of the pellicle elastic modulus, as the modulus of the RΔ*rbmC* pellicle closely follows that of the rugose (Fig. 2 *B*). In fact, the macroscale appearances of the rugose and RΔ*rbmC* pellicles are very similar throughout growth (Fig. 2 *A*). This suggests that in comparison to other matrix proteins, RbmC is not required for providing mechanical strength to the *V. cholerae* pellicle or in determining its macroscale structure in the rugose genetic background.

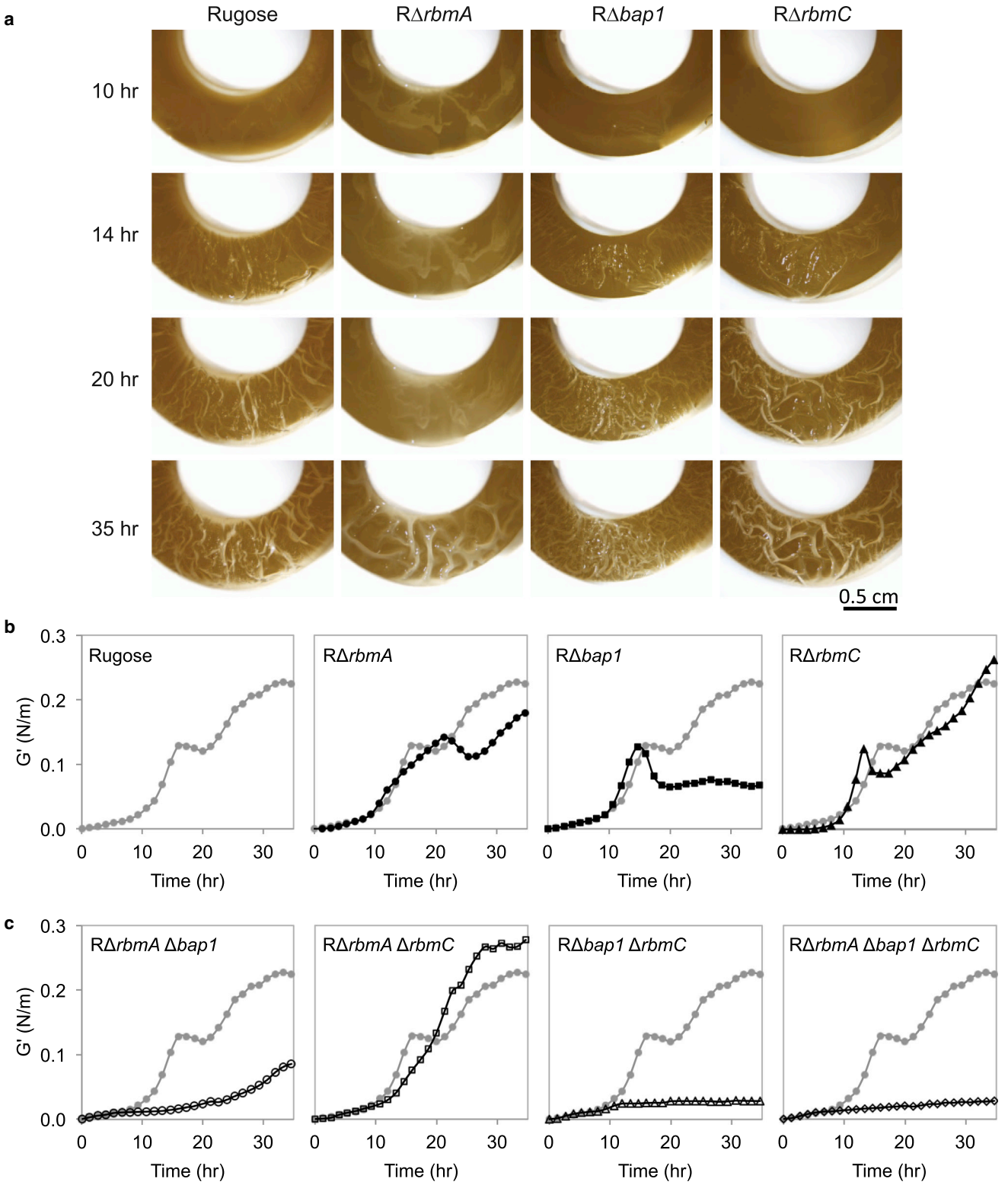

FIGURE 2 (*a*) Rugose, RΔ*rbmA*, RΔ*bap1*, and RΔ*rbmC* pellicles growing in the Teflon flow cell over time. The images were captured without the du Noüy ring for easy visualization. (*b*) Evolution of the interfacial elastic moduli of the rugose, RΔ*rbmA*, RΔ*bap1*, and RΔ*rbmC* pellicles. The rugose data is shown in the leftmost plot; subsequent plots compare the mutant data (*black*) to the rugose parent strain (*gray*). The data shown is representative of three trials. (*c*) Evolution of the interfacial elastic moduli of the RΔ*rbmA*Δ*bap1*, RΔ*rbmA*Δ*rbmC*, RΔ*bap1*Δ*rbmC*, and RΔ*rbmA*Δ*bap1*Δ*rbmC* pellicles (*black*) referenced to the rugose pellicle (*gray*). The data shown is representative of three trials. To see this figure in color, go online.

To test whether the abundance of each matrix protein correlates with the timing of the local maximum, we determined RbmA, RbmC, and Bap1 levels from planktonic cells and pellicle samples collected after 10, 12, 15, and 20 h of incubation grown in the same Teflon cells that the rheological measurements were performed in (Fig. 3). Although no significant changes were observed for RbmC and Bap1 levels, abundance of full-length RbmA in the pellicle is reduced at 20 h. At 15 and 20 h, we also observed that a processed form of RbmA is present in the pellicle. These observations suggest that the levels of RbmA, Bap1, and RbmC do not change significantly when the local maximum occurs at 14 h, and that the full-length RbmA may not be important for subsequent pellicle formation in later stages. However, for all pellicles, we did observe a correlation between the local maximum in each measurement and the change in pellicle appearance, i.e., all pellicles appear smooth before the time corresponding to the local maximum in G′, whereas they wrinkle after passing the local maximum.

Bap1 contributes significantly to pellicle elasticity

To investigate the combinatorial effect of matrix proteins and to further test the potential requirement of Bap1 for mature pellicle formation and elasticity, we generated and measured the elastic moduli of the double mutants RΔ*rbmA*Δ*bap1*, RΔ*rbmA*Δ*rbmC*, and RΔ*bap1*Δ*rbmC*, and the triple mutant RΔ*rbmA*Δ*bap1*Δ*rbmC* (Fig. 2 *C*). Two of these mutants that lack Bap1, RΔ*bap1*Δ*rbmC* and RΔ*rbmA*Δ*bap1*Δ*rbmC* do not form a pellicle in the flow cell used in this study and generate a negligible elastic modulus over the 30-h time course. RΔ*rbmA*Δ*bap1* is capable of forming only a weak pellicle with delayed kinetics compared to the rugose pellicle, demonstrating additive properties of the delayed development of the RΔ*rbmA* pellicle and low elastic modulus of the RΔ*bap1* pellicle. Finally, RΔ*rbmA*Δ*rbmC* was capable of forming a pellicle with an elastic modulus similar to that of rugose, although the modulus did not exhibit a local maximum as observed for rugose and single mutant pellicles. Thus, these results provide further support for the significant role and requirement of Bap1 in the development and maintenance of pellicle elasticity.

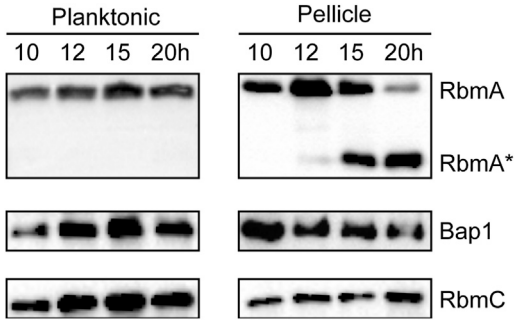

FIGURE 3 Western blot analyses on RbmA, Bap1, and RbmC in planktonic and pellicle samples. Planktonic and pellicle samples collected at 10, 12, 15, and 20 h were analyzed for the abundance of RbmA, Bap1, and RbmC. The full-length RbmA is processed to a smaller species (RbmA*). Western blot shown is a representative of four biological replicates.

Bap1 contributes significantly to pellicle hydrophobicity

In working with rugose and mutant pellicles, we observed additional informative macroscopic properties. Fig. 4 *A* presents rugose and single mutant pellicles that were grown in a 24-well dish for 48 h. These pellicles were removed from their original wells and transferred to new wells filled with deionized water. When transferring the pellicles, the rugose, RΔ*rbmA*, and RΔ*rbmC* pellicles instantly spread to their original form upon contact with the air-water interface. In contrast, the RΔ*bap1* pellicle curled upon itself and sank below the surface. From this qualitative observation, we hypothesized that Bap1 provides the *V. cholerae* pellicle

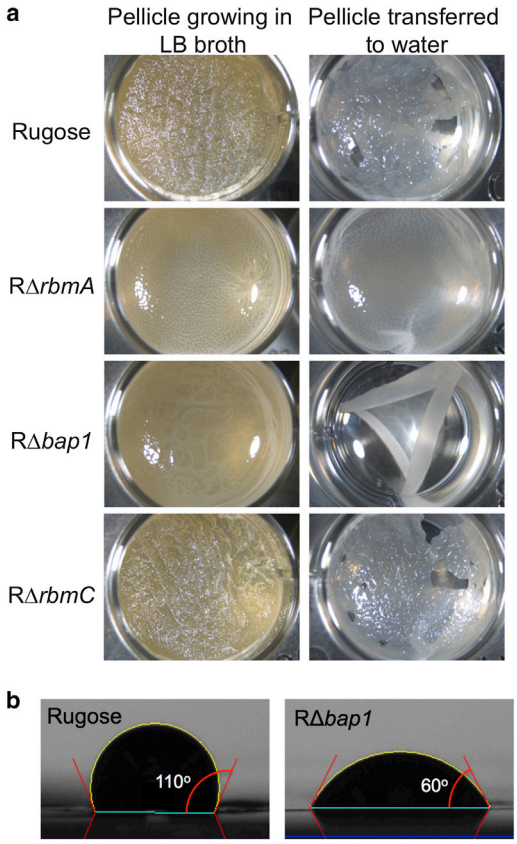

FIGURE 4 (*a*) Rugose, RΔ*rbmA*, RΔ*bap1*, and RΔ*rbmC* pellicles growing in a 24-well dish and then transferred to a 24-well dish containing deionized water. Note that upon transferring, the rugose, RΔ*rbmA*, and RΔ*rbmC* pellicles remain at the air-liquid interface, but the RΔ*bap1* pellicle curls upon itself and sinks to the bottom of the well. (*b*) Contact angle measurements on dry rugose and RΔ*bap1* pellicles. Multiple measurements gave a contact angle of 100° ± 10° for the rugose pellicle and 50° ± 10° for the RΔ*bap1* pellicle, indicating that the RΔ*bap1* pellicle is more hydrophilic. To see this figure in color, go online.

with hydrophobic character that allows the pellicle to spread and remain at an air-water interface.

We therefore used contact angle measurements to quantify the hydrophobic-hydrophilic nature of the rugose and RΔ*bap1* pellicles. Briefly, to determine the contact angle, a drop of water is placed on a surface and the angle between the air-liquid interface and solid surface is measured. A larger contact angle indicates that the surface of interest is more hydrophobic; conversely, a smaller angle indicates that the surface is more hydrophilic as the water droplet spreads farther. Our measurements on dry pellicles placed on glass slides yielded a contact angle of 100° ± 10° for rugose and 50° ± 10° for RΔ*bap1*, with representative images provided in Fig. 4 *B*. This confirmed our hypothesis that the RΔ*bap1* pellicle is more hydrophilic and shows that Bap1 contributes hydrophobicity to the rugose pellicle.

Mature rugose and mutant pellicles exhibit different microscale architectures

To further examine the differences underlying the correlated macroscopic and mechanical properties of the rugose and mutant pellicles, we used SEM to investigate their microscale architecture. Images were captured at two different length scales to examine the overall pellicle structure (Fig. 5) and, at higher magnification, features at the cellular level (Fig. 6). As shown in Fig. 5, we observed two surfaces

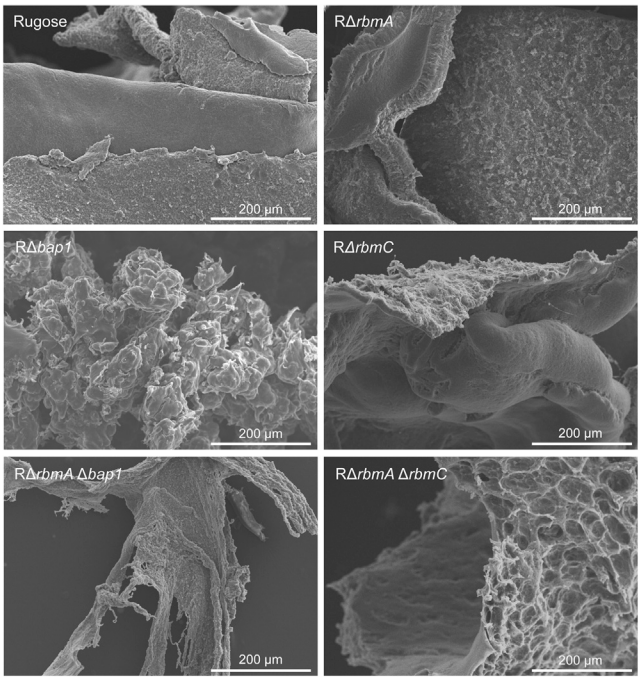

FIGURE 5 SEM images of the rugose and mutant pellicles. Note the dual-sided architecture of the rugose, RΔ*rbmA*, RΔ*rbmC*, and RΔ*rbmA* ΔrbmC pellicles with both rough and smooth sides. The RΔ*bap1* and RΔ*rbmA*Δ*bap1* pellicles were more amorphous and did not display these distinctly different surfaces.

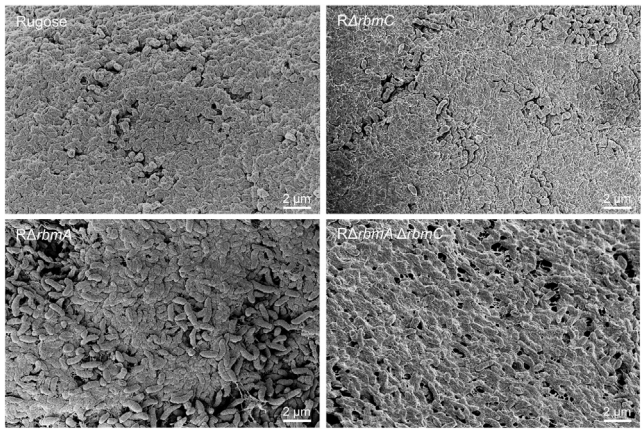

FIGURE 6 SEM images of the smoother pellicle surface (observed in Fig. 5) taken at higher magnification for the rugose, RΔ*rbmA*, RΔ*rbmC*, and RΔ*rbmA*Δ*rbmC* pellicles. For the rugose and RΔ*rbmC* pellicle this surface is similar and appears more compact. For the RΔ*rbmA* and RΔ*rbmA*Δ*rbmC* this surface is less compact, and individual bacteria and strands of extracellular matrix are distinguishable.

of different texture in the rugose pellicle. This dual-sided architecture is also apparent for the RΔ*rbmA*, RΔ*rbmC*, and RΔ*rbmA*Δ*rbmC* pellicles. In contrast, we did not observe these distinct surfaces in the RΔ*bap1* or RΔ*rbmA*Δ*bap1* pellicles. Thus, Bap1 is required for the development of this dual-sided pellicle architecture and, considering the panel of mutants, pellicles lacking Bap1 have a microscale architecture that differs the most from the rugose pellicle.

At higher magnifications, the rough sides of the rugose, RΔ*rbmA*, RΔ*rbmC*, and RΔ*rbmA*Δ*rbmC* pellicles are similar; however, we observed differences in the appearance of the smooth sides of these pellicles (Fig. 6). In the rugose and RΔ*rbmC* pellicles, the smooth sides are similar and appear highly compact. In the RΔ*rbmA* and RΔ*rbmA* Δ*rbmC* pellicles, the smooth side is less compact, and some individual bacteria and strands of extracellular matrix are visible. Thus, pellicles lacking RbmC alone do not have a significantly different architecture compared to the rugose pellicle, although pellicles lacking RbmA are different at the microscale.

DISCUSSION

Biofilms are linked to a variety of adverse consequences in industrial settings and in human health, and effective strategies are needed to prevent and disperse biofilms. This is a particularly challenging task, considering that biofilms are complex and heterogeneous structures with properties that evolve as a function of time and space. Thus, new methods are needed to probe and measure the fundamental physical and chemical properties of bacterial biofilms. Sensitive measurements of mechanical properties can lend insight into biofilm architecture, as properties such as elasticity result from the composition and structure of the material.

In our work here with *V. cholerae*, we discovered that interfacial rheology measurements were crucial in extending the qualitative observations of macroscopic pellicle morphology and visualization by electron microscopy to understand the molecular basis of pellicle phenotypes. Moreover, tracking the evolution of elasticity in real time reveals the dynamics of biofilm formation and the temporal contributions of different matrix components.

As a general phenomenon, we discovered that all pellicles exhibit a transition from a visually apparent smooth collection of bacteria at the air-liquid interface, at time points before the elastic modulus passes a characteristic local maximum, to a more wrinkled film at time points after the local maximum is observed. This is emphasized by the RΔ*rbmA* pellicle, which exhibits a delayed local maximum relative to the rugose pellicle (22 h versus 14 h) and, correspondingly, begins to wrinkle considerably only after 22 h. Additionally, the double mutants that do form pellicles (RΔ*rbmA*Δ*bap1* and *R*Δ*rbmA*Δ*rbmC*) do not wrinkle and their elastic moduli do not pass through local maxima. These observations support the notion that pellicle wrinkling may be attributed to a buckling instability (theory developed by Trejo et al. (27)) through which the pellicle buckles vertically to relieve the compressive stresses that arise upon fully occupying the surface area in the confined container. In further support of this, the local maximum exhibited by each pellicle, regardless of its timing, corresponds to a similar elastic modulus of ~0.12 N/m, a threshold elasticity that must be reached before wrinkling occurs. Additionally, softer pellicles with lower elastic moduli are predicted to have smaller wrinkles (27). Indeed, the RΔ*bap1* pellicle with a lower elastic modulus harbors smaller wrinkles than the rugose pellicle. Therefore, we propose that the local maxima report the onset of buckling, where buckling causes a transient decrease in pellicle mechanical lateral strength. The phenomenon of wrinkling is also of physiological significance and can be beneficial for bacterial survival; for example, the wrinkles of *Bacillus subtilis* biofilms create a network of channels that enhance liquid transport and therefore transport of nutrients, waste, and signaling molecules (28). The roughness of the biofilm surface may also help repel liquid antimicrobials (29). Therefore, although the *V. cholerae* pellicle may momentarily experience a decrease in its mechanical integrity, it may be ultimately beneficial to undergo this wrinkling transition.

From our integrated approach to examine the molecular contributions of matrix proteins to pellicle architecture and mechanical integrity, we found that RbmC is dispensable for the formation of pellicles in the rugose genetic background. We observed that the absence of RbmC does not significantly affect the kinetics of growth, the mechanical strength, or the structure of the *V. cholerae* pellicle. However, it is important to note that although RbmC alone does not have a major impact on pellicle formation, a striking loss of pellicle formation was observed for cells lacking both Bap1 and RbmC. Based on the panel of single and double mutant pellicle rheology, we observe that a lack of RbmC can be compensated for by the presence of Bap1. This compensation is consistent with Bap1 and RbmC sharing 47% peptide sequence similarity (12), allowing them to potentially share structural roles. However, the absence of Bap1 significantly decreases pellicle elasticity. Thus, the inability of RbmC to partially complement pellicle formation in the absence of Bap1 shows that they are not entirely functionally identical in contributing to pellicle architecture.

In the absence of RbmA, subtle differences were observed that are consistent with its proposed role in cell-to-cell adhesion (14). Pellicles lacking RbmA exhibit a delayed evolution of pellicle formation, wrinkling, and elasticity and, although the pellicles still display dual-sided textural distinctions, the smoother side of the RΔ*rbmA* pellicles is less compact than the rugose pellicle. Additionally, at times after the local maximum in elasticity and development of wrinkled morphology in the rugose pellicle, the level of RbmA in the pellicle decreases and a processed form of RbmA is more prevalent, suggesting that the full-length RbmA may be necessary only for the initial stages of pellicle formation, whereas the processed-form of RbmA is involved in later stages of pellicle formation. Thus, RbmA is important in the early stages of *V. cholerae* pellicle development and in generating a wrinkled morphology.

The most dramatic effects on pellicle morphology and elasticity were observed in the absence of Bap1. The RΔ*bap1* pellicle does not attain the high value of elasticity associated with the rugose pellicle and does not exhibit the broad wrinkles and wave-like appearance of the rugose pellicle. Instead, it displays small densely packed shallow wrinkles, does not display the two-sided textural distinctions and is more amorphous, lacking the smooth surface exhibited by other pellicles. Additionally, the RΔ*bap1* pellicle does not easily spread and remain at the air-water interface and contact angle measurements revealed that this is attributed to increased hydrophilicity relative to the rugose pellicle. Thus, among the matrix proteins, Bap1 is the most critical molecular determinant of pellicle mechanical strength and hydrophobicity, especially crucial in later stages of growth.

CONCLUSIONS

Overall, our measurements provide fundamental physicochemical data correlating the microscale architecture, macroscale morphology, and mechanical properties of rugose and mutant *V. cholerae* pellicles. By investigating the interfacial properties of pellicles formed by mutants deficient in one or more extracellular matrix proteins, we discovered that RbmA is important in the early stages of pellicle growth, whereas Bap1 is more important for maintaining pellicle strength. Bap1 is required for rugose pellicle morphology, contributes significantly to pellicle

hydrophobicity, and is required to maintain pellicle stability and integrity at the air-liquid interface. These findings, together with the dramatic changes in the microscale architecture of the pellicle, emphasize the significant role of Bap1 in the development and maintenance of *V. cholerae* pellicle strength. Thus, Bap1 is an attractive target for the prevention and dispersal of *V. cholerae* biofilms. Similarly, in previous work on solid surfaces, Bap1 was found concentrated at the biofilm-surface interface. More generally, hydrophobic extracellular structures are also prevalent in the extracellular matrix of other organisms, for example the chaplins from *Streptomyces* spp (30), curli and tafi amyloids from *E. coli* and *Salmonella* spp (30), hydrophobins from filamentous fungi (31), the TasA amyloids (32), and the matrix protein BslA in *Bacillus subtilis* (33). We suggest that the presence of hydrophobic components in the extracellular matrix of any biofilm former may be necessary for pellicle formation. Thus, extracellular hydrophobic proteins present in other species may also represent appropriate targets for drug discovery efforts directed toward the prevention and elimination of harmful bacterial biofilms.

We thank the Cell Sciences Imaging Facility at Stanford (Lydia Joubert) for assistance with electron microscopy. Additionally, we thank the Bao Research Group at Stanford (Yeongin Kim) for use of the contact angle goniometer and assistance with measurements.

This work was supported by awards from The Center for Molecular Analysis and Design to E.C.H. and National Institutes of Health (NIH) (R01AI055987) to F.H.Y. L.C. acknowledges support from the NIH Director's New Innovator Award (DP2OD007488).

REFERENCES

1. Harris, J. B., R. C. LaRocque, …, S. B. Calderwood. 2012. Cholera. *Lancet.* 379:2466–2476.
2. Charles, R. C., and E. T. Ryan. 2011. Cholera in the 21st century. *Curr. Opin. Infect. Dis.* 24:472–477.
3. Nelson, E. J., J. B. Harris, …, A. Camilli. 2009. Cholera transmission: the host, pathogen and bacteriophage dynamic. *Nat. Rev. Microbiol.* 7:693–702.
4. Faruque, S. M., M. J. Albert, and J. J. Mekalanos. 1998. Epidemiology, genetics, and ecology of toxigenic *Vibrio cholerae*. *Microbiol. Mol. Biol. Rev.* 62:1301–1314.
5. Yildiz, F. H., and G. K. Schoolnik. 1999. *Vibrio cholerae* O1 El Tor: identification of a gene cluster required for the rugose colony type, exopolysaccharide production, chlorine resistance, and biofilm formation. *Proc. Natl. Acad. Sci. USA.* 96:4028–4033.
6. Watnick, P. I., and R. Kolter. 1999. Steps in the development of a *Vibrio cholerae* El Tor biofilm. *Mol. Microbiol.* 34:586–595.
7. Huq, A., C. A. Whitehouse, …, R. R. Colwell. 2008. Biofilms in water, its role and impact in human disease transmission. *Curr. Opin. Biotechnol.* 19:244–247.
8. Lutz, C., M. Erken, …, D. McDougald. 2013. Environmental reservoirs and mechanisms of persistence of *Vibrio cholerae*. *Front. Microbiol.* 4:375.
9. Alam, M., M. Sultana, …, R. R. Colwell. 2007. Viable but nonculturable *Vibrio cholerae* O1 in biofilms in the aquatic environment and their role in cholera transmission. *Proc. Natl. Acad. Sci. USA.* 104:17801–17806.
10. Faruque, S. M., K. Biswas, …, J. J. Mekalanos. 2006. Transmissibility of cholera: in vivo-formed biofilms and their relationship to infectivity and persistence in the environment. *Proc. Natl. Acad. Sci. USA.* 103:6350–6355.
11. Fong, J. C., K. Karplus, …, F. H. Yildiz. 2006. Identification and characterization of RbmA, a novel protein required for the development of rugose colony morphology and biofilm structure in *Vibrio cholerae*. *J. Bacteriol.* 188:1049–1059.
12. Fong, J. C., and F. H. Yildiz. 2007. The *rbmBCDEF* gene cluster modulates development of rugose colony morphology and biofilm formation in *Vibrio cholerae*. *J. Bacteriol.* 189:2319–2330.
13. Fong, J. C., K. A. Syed, …, F. H. Yildiz. 2010. Role of *Vibrio* polysaccharide (vps) genes in VPS production, biofilm formation and *Vibrio cholerae* pathogenesis. *Microbiology.* 156:2757–2769.
14. Berk, V., J. C. Fong, …, S. Chu. 2012. Molecular architecture and assembly principles of *Vibrio cholerae* biofilms. *Science.* 337:236–239.
15. Absalon, C., K. Van Dellen, and P. I. Watnick. 2011. A communal bacterial adhesin anchors biofilm and bystander cells to surfaces. *PLoS Pathog.* 7:e1002210.
16. Bos, M. A., and T. van Vliet. 2001. Interfacial rheological properties of adsorbed protein layers and surfactants: a review. *Adv. Colloid Interface Sci.* 91:437–471.
17. Olson, D. J., and G. G. Fuller. 2000. Contraction and expansion flows of Langmuir monolayers. *J. Non-Newton Fluid Mech.* 89:187–207.
18. Reynaert, S., P. Moldenaers, and J. Vermant. 2006. Control over colloidal aggregation in monolayers of latex particles at the oil-water interface. *Langmuir.* 22:4936–4945.
19. Fuller, G. G., and J. Vermant. 2012. Complex fluid-fluid interfaces: rheology and structure. *Annu. Rev. Chem. Biomol. Eng.* 3:519–543.
20. Wu, C., J. Y. Lim, …, L. Cegelski. 2012. Quantitative analysis of amyloid-integrated biofilms formed by uropathogenic *Escherichia coli* at the air-liquid interface. *Biophys. J.* 103:464–471.
21. Wu, C., J. Y. Lim, …, L. Cegelski. 2013. Disruption of *Escherichia coli* amyloid-integrated biofilm formation at the air-liquid interface by a polysorbate surfactant. *Langmuir.* 29:920–926.
22. Patrick, A. R., B. Lukas, …, F. Peter. 2013. In-situ quantification of the interfacial rheological response of bacterial biofilms to environmental stimuli. *PLoS ONE.* 8:e78524.
23. Vandebril, S., A. Franck, …, J. Vermant. 2010. A double wall-ring geometry for interfacial shear rheometry. *Rheol. Acta.* 49:131–144.
24. Lieleg, O., M. Caldara, …, K. Ribbeck. 2011. Mechanical robustness of *Pseudomonas aeruginosa* biofilms. *Soft Matter.* 7:3307–3314.
25. Pavlovsky, L., J. G. Younger, and M. J. Solomon. 2013. In situ rheology of *Staphylococcus epidermidis* bacterial biofilms. *Soft Matter.* 9:122–131.
26. Dahlbäck, B., M. Hermansson, …, B. Norkrans. 1981. The hydrophobicity of bacteria - an important factor in their initial adhesion at the air-water interface. *Arch. Microbiol.* 128:267–270.
27. Trejo, M., C. Douarche, …, E. Raspaud. 2013. Elasticity and wrinkled morphology of *Bacillus subtilis* pellicles. *Proc. Natl. Acad. Sci. USA.* 110:2011–2016.
28. Wilking, J. N., V. Zaburdaev, …, D. A. Weitz. 2013. Liquid transport facilitated by channels in *Bacillus subtilis* biofilms. *Proc. Natl. Acad. Sci. USA.* 110:848–852.
29. Epstein, A. K., B. Pokroy, …, J. Aizenberg. 2010. Bacterial biofilm shows persistent resistance to liquid wetting and gas penetration. *Pro. Natl. Acad. Sci. USA.* 108:995–1000.
30. Gebbink, M. F., D. Claessen, …, H. A. Wösten. 2005. Amyloids—a functional coat for microorganisms. *Nat. Rev. Microbiol.* 3:333–341.
31. Wösten, H. A. 2001. Hydrophobins: multipurpose proteins. *Annu. Rev. Microbiol.* 55:625–646.
32. Romero, D., C. Aguilar, …, R. Kolter. 2010. Amyloid fibers provide structural integrity to *Bacillus subtilis* biofilms. *Proc. Natl. Acad. Sci. USA.* 107:2230–2234.
33. Kobayashi, K., and M. Iwano. 2012. BslA(YuaB) forms a hydrophobic layer on the surface of *Bacillus subtilis* biofilms. *Mol. Microbiol.* 85:51–66.